*Polish Journal of Chemical Technology, 12, **2**, 18 — 28, 2010, 10.2478/v10026-010-0013-2*

Parametric studies and simulation of PSA process for oxygen production from air

Ankit K. Beeyani[1a], Kailash Singh[2a], Raj K. Vyas[a*], Shashi Kumar[3b], Surendra Kumar[4b]

[a]*Malaviya National Institute of Technology, Department of Chemical Engineering, Jaipur-302 017, India*
[b]*Indian Institute of Technology, Department of Chemical Engineering, Roorkee-247 667, India*
[1]*biyaniankitkumar@gmail.com,* [2]*ksingh.mnit@gmail.com,* [3]*sashifch@iitr.ernet.in,* [4]*skumar@iitr.ernet.in*
[*]*Corresponding author: e-mail: rkvyas2@gmail.com*

A numerical simulation and parametric studies for the separation of air using 5A zeolite for the production of oxygen are presented for a basic two bed pressure swing adsorption (PSA) process. The simulation is based on an in-house program 'PSASOL' developed in MATLAB®. The transient process of PSA has been described by a set of partial differential equations, which were solved using a finite difference method. Simulation results have been validated with the experimental data from literature.
Based on the simulation results, an optimal set of operational parameter values has been obtained for the PSA bed. The values of the optimal parameters, viz. adsorption pressure, cycle time, feed rate, and product rate have been found to be 2.5 atm, 150 s, 15 cm^3/s, and 2.55 cm^3/s, respectively. For the optimal conditions, purity of 95.45% and recovery of 77.3% have been achieved. It has also been found that a longer tubular unit with the length to diameter (L/D) ratio of 10.5 is advantageous. The estimated pressure drop across the bed has been found to be negligible. Power consumption and productivity have also been computed.

Keywords: Pressure swing adsorption, mathematical model, simulation, oxygen production, MATLAB, Zeolite 5A.

INTRODUCTION

Several industrial processes require oxygen with the purity more than 90%. Applications of enriched oxygen include enhanced combustion in glass furnaces, electric arc furnaces, oxygen bleaching in pulp and paper industries, cement industry, wastewater treatment, fish farming, environmental remediation, glass-blowing, oxygen bar, medical use, and hydrogen production from methanol reformats in fuel cells[1 – 4]. Recently, because of the reduction and sequestration of CO_2, O_2 inhalation combustion processes have been developed extensively for use in the iron, steel, and incineration industries. In these industries, O_2 needs to be at least 95% pure (high purity O_2) to be used cost-effectively in fuel combustion because of the carbon tax placed on CO_2 capturing[5]. A major advantage of pressure swing adsorption (PSA) process relative to other adsorption processes, such as temperature swing adsorption, is that the pressure can be changed much more rapidly than the temperature, thus making it possible to operate a PSA process on a much faster cycle, thereby increasing throughput per unit of adsorbent bed volume. Thus, pressure controlled PSA is easy to operate and control[6].

Cryogenic processes for oxygen production are highly efficient and are quite common, particularly for large-volume applications. However, the PSA process, which was originally developed by Skarstrom has become a widely used unit operation for gas separation or purification nowadays[4]. The process runs continuously with automatic regeneration of the adsorbent. PSA is attractive, particularly at low throughput rate as the unit is compact and requires no heating for desorption step. PSA has also an economic edge over cryogenic process.

The adsorption materials used in oxygen production include a variety of zeolites, e.g. 13X, 10X, 4A, 5A, LiX, LiLSX, LiAgX etc., which selectively adsorb nitrogen, moisture, and carbon dioxide gas, while allowing oxygen molecules to pass through the unit[2, 3, 5, 7 – 10]. The simulation of O_2 production by PSA process from air has been studied earlier also[11 – 13]. In the earlier studies, the effect of adsorption pressure, cycle time, adsorption duration, feed flow rate, and the product flow rate have been studied on product purity and recovery. Cruz *et* al.[14] proposed the adaptive multiresolution approach for the optimization of general cyclic adsorption separation processes using Skarstrom cycle with pressure equalization. Furthermore, the optimal operating conditions were determined for a single bed over a single cycle of operation by Nilchan and Pantelides[15]. The work done by Nilchan and Pantelides is remarkable in respect of rapid pressure swing adsorption (RPSA) process, however, it did not consider argon, which is also present in the air (1% approx.). Moreover, the dynamic simulation results have been compared with those using complete discretization by the authors for a single bed. The results of the simulation have not been compared with any experimental data. In the present study, simulation has been done for a single bed with the presence of argon in feed air and the simulated results have been validated with the reported experimental data.

A few other studies on the optimization of design have also been made earlier[16, 17]. One of the design variables, Length to diameter (L/D) ratio is also important for the economic design of the PSA system, as it determines the dispersion of feed across the bed radius and hence, affects purity and recovery. L/D ratio has been studied earlier also by Nikolic *et* al.[18], however, the study was based on hydrogen recovery using a layered PSA bed. Moreover, the effect of purge to feed velocity ratio (G) on the time to achieve cyclic steady state was not studied; however, G has its influence on the minimum number of cycles to achieve cyclic steady state.

In the present work, a basic two bed Skarstrom cycle using 5A zeolite has been simulated for the production of

O_2 from air using the PSA process. The results of simulation have been validated with the experimental data available in literature. Further, the effects of total cycle time, adsorption pressure, feed flow rate, the product rate and the *L/D* ratio on the product purity and recovery have been studied and the optimal values of these process variables have been found out in order to maximize the product purity and recovery.

Though, simulation of O_2 production from air using PSA has been studied earlier also, the present work employs an in-house developed MATLAB based program for this purpose. MATLAB based simulation for PSA process has been scarcely reported. This work utilizes a simple simulation methodology using partial differential equations taken from literature to represent the Skarstrom cycle based PSA process. MATLAB has the solvers for stiff problems such as *ode15s,* which also allows the solution of Differential-Algebraic Equations (DAEs). Linear algebra and the built-in array operations are relatively fast in MATLAB and in particular it is easy to exploit sparse jacobians[19]. It has been reported that by default *ode15s* approximates the jabian matrix numerically. It handles the matrix much more efficiently as compared to most of other stiff solvers[20].

MATHEMATICAL MODEL

PSA processes are transient in nature due to continuous adsorption/desorption of the adsorbate. The operation of four steps PSA process is described elsewhere[21, 22]. Such processes are described by a set of partial differential equations, which require an appropriate solution procedure. A number of simplifying assumptions have been made for a two bed process operating with Skarstrom cycle.

Assumptions

1. The system is considered to be isothermal.
2. The ideal gas law applies.
3. Frictional pressure drop through the bed is negligible.
4. Total pressure in the bed is assumed constant during adsorption and purge steps.
5. During pressurization and blowdown, the total pressure in the bed varies linearly with time.
6. The fluid velocity within the bed during adsorption and desorption varies along the length of the column, as determined by the mass balance.
7. The flow pattern is represented by the axial dispersion model.
8. The equilibrium relationship for both components is represented by binary Langmuir isotherm.
9. It is assumed that argon and oxygen have the same equilibrium isotherms[22] and therefore, the ratio of argon/oxygen remains the same as in the feed.
10. The mass transfer rate is represented by a linearized driving force (LDF) expression.

In a commercial operation, the feed stream would be supplied by a compressor, hence a constant flow situation is probably more appropriate rather than a constant pressure feed stream. Therefore, during pressurization the inlet velocity, *v*, changes with changing the column pressure.

The equations describing the cyclic operation are as follows[21, 23]:

Material balance for component *i* in bulk phase:

$$-D_L \frac{\partial^2 c_i}{\partial z^2} + v\frac{\partial c_i}{\partial z} + c_i \frac{\partial v}{\partial z} + \frac{\partial c_i}{\partial t} + \left(\frac{1-\varepsilon}{\varepsilon}\right)\frac{\partial q_i}{\partial t} = 0 \quad (1)$$

Continuity condition:

$$\sum_i c_i = C \neq f(z)$$

$$= f(t); \quad \text{pressurization and blowdown}$$

$$\neq f(t); \quad \text{adsorption and purge} \quad (2)$$

Overall material balance:

$$C\frac{\partial v}{\partial z} + \frac{\partial C}{\partial t} + \frac{1-\varepsilon}{\varepsilon}\sum_i \frac{\partial q_i}{\partial t} = 0 \quad (3)$$

Mass transfer rates:

$$\frac{\partial q_i}{\partial t} = k_i\left(q_i^* - q_i\right) \quad (4)$$

Adsorption equilibrium:

$$\frac{q_i^*}{q_{is}} = \frac{b_i c_i}{1+\sum_i b_i c_i} \quad (5)$$

Boundary conditions for pressurization, adsorption, and purge:

$$D_L \left.\frac{\partial c_i}{\partial z}\right|_{z=0} = -v_0\left(c_i\big|_{z=0^-} - c_i\big|_{z=0}\right); \quad \left.\frac{\partial c_i}{\partial z}\right|_{z=L} = 0 \quad (6)$$

$$\left(c_i\big|_{z=0^-}\right)_{purge} = \frac{P_L}{P_H}\left(c_i\big|_{z=L}\right)_{Adsorption} \quad (7)$$

Blowdown:

$$\left.\frac{\partial c_i}{\partial z}\right|_{z=0} = 0 \; ; \quad \left.\frac{\partial c_i}{\partial z}\right|_{z=L} = 0 \quad (8)$$

Velocity boundary conditions:

$$v\big|_{z=0} = v_0 \text{, Pressurization} \quad (9a)$$

$$= v_{0H} \text{, High-Pressure Adsorption} \quad (9b)$$

$$\left.\frac{\partial v}{\partial z}\right|_{z=0} = 0\text{, Blowdown and Purge} \quad (9c)$$

$$\left.\frac{\partial v}{\partial z}\right|_{z=L} = 0\text{, Adsorption and Pressurization} \quad (10a)$$

$$v\big|_{z=L} = 0 \text{, Blowdown} \quad (10b)$$

$$v\big|_{z=L} = -Gv_{0H} \text{, Purge} \quad (10c)$$

Initial conditions: saturated bed

$$c_i(z,0) = c_{i,0}; \quad q_i(z,0) = q_i^* \quad (11)$$

Equations (1) to (11) were rearranged and rewritten using central finite difference. A program 'PSASOL' was written in MATLAB® to solve these simultaneous equations. The initial condition has been taken corresponding to the saturated bed with bulk concentration as the feed composition. The final CSS will not differ, if we assume a different initial condition (such as clean bed). The design and operating variables are given in Table 1.

Two parameters of PSA system, viz., product purity and percent recovery of O_2 have been studied. Recovery measures the amount of component that is contained in the product stream divided by the amount of the same com-

Table 1. Data used in simulation[12]

Parameter	Value
Feed Composition	21% Oxygen, 78% Nitrogen, and 1% Argon
Adsorbent	5A
Bed length (L), cm	35
Bed diameter, cm	3.5
Particle diameter (d_p), cm	0.0707
Bed voidage (ε)	0.4
Ambient temperature, °C	25
Blowdown pressure, atm	1.0
Purge Pressure (P_L), atm	1.07
Axial Dispersion Coefficient (D_L), m^2/s	2.63×10^{-5}
Duration of adsorption and purge steps	20% of total cycle time
Duration of blowdown and pressurization steps	30% of total cycle time
Equilibrium constant for oxygen (K_A)	4.7
Equilibrium constant for nitrogen (K_B)	14.8
LDF constant for O_2 (k_A), s^{-1}	62.0 (at 1 atm)
LDF constant for N_2 (k_B) s^{-1}	19.7 (at 1 atm)
Saturation constant for oxygen (q_{AS}), mol/cm^3	5.26×10^{-3}
Saturation constant for nitrogen (q_{BS}), mol/cm^3	5.26×10^{-3}

ponent in the feed mixture. Percent recovery of O_2 is calculated using the following expression[23]:

$$\text{Percent recovery} = \frac{\int_0^{t_{ads}} y_{O_2,exit} F_{product} dt}{\int_0^{t_{ads}} y_{O_2,feed} F_{feed} dt} \times 100 \quad (12)$$

Product Purity gives an idea about percentage of desired component in the product stream. Average purity of O_2 in the product has been expressed as the mole percent of O_2 using the following expression[23]:

$$\text{Average percent product purity} = \frac{\int_0^{t_{ads}} y_{O_2} dt}{t_{ads}} \times 100 \quad (13)$$

SOLUTION METHODOLOGY

Modeling of pressure swing adsorption involves partial differential equations (PDEs) in time and space with periodic boundary conditions that link the processing steps together. The solution of this coupled stiff PDE system is governed by steep fronts moving with time[24]. An analytical solution of these partial differential equations is difficult; therefore, the numerical method using finite difference technique was used to solve these equations to obtain the product purity, recovery, and concentration profile along the bed.

The partial differential equations were first converted into ordinary differential equations-initial value problems (ODE-IVPs) by discretization along the bed length. After discretization, a set of differential-algebraic equations (DAEs) were obtained. The number of differential and algebraic equations so formed were $4N_{FD}$ and $N_{FD}+5$, respectively, which comes out to 800 and 205, respectively for 200 finite difference intervals, where N_{FD} is the number of finite difference intervals. Mass matrix was defined to differentiate the differential and algebraic equations, which is required in the MATLAB® function *ode15s* for solving DAEs. After several runs, the optimum number of finite difference intervals was found to be 100 – 200 required for reasonable accuracy. The four different stages of operation, viz. adsorption, blowdown, purge, and pressurization have different boundary conditions as mentioned in the model, therefore, the PDEs were solved successively for these stages in each cycle using inbuilt function *ode15s* in MATLAB®. After a few cycles (15 – 30 cycles), a new steady state, the so-called cyclic steady state (CSS) is achieved, after which, there is no more change in average product purity and recovery. As the finite-difference technique was used to discretize the PDEs along the bed length, sparse matrices were formed. Therefore, to save computation time, Jacobian pattern (*JPattern*) was defined in MATLAB® program. Despite the use of *JPattern* the average run time for the developed program was 4 min per cycle for the model using 200 finite difference intervals along the bed length on an Intel Core Duo, 1.86 GHz processor with 1 GB RAM machine. The flow chart of the simulation methodology is shown in Figure 1.

RESULTS AND DISCUSSION

PSASOL developed in this work was run for several experimental data sets of Farooq *et al.*[12]. The simulated results obtained were validated with experimental results as shown in Figure 2(a) and (b). The figures also show the simulated results of Farooq *et al.*[12] in which they used orthogonal collocation (OC) method with 5 internal OC points for solving the unsteady state partial differential equations. However, the orthogonal collocation method does not show any significant advantage when a large number of OC points are used along the spatial direction as the OC points start accumulating near the boundaries. Moreover, as the *moving steep concentration changes* exist inside the bed, the OC method may not give accurate location of the point of steep change. Orthogonal collocation with finite elements (OCFE) technique was not used as significant improvement in terms of computational time was not expected as compared to finite difference (FD) method. In the current work only FD method with fine mesh grid (200 FD intervals) was used to solve the model equations. It was found that the simulated re-

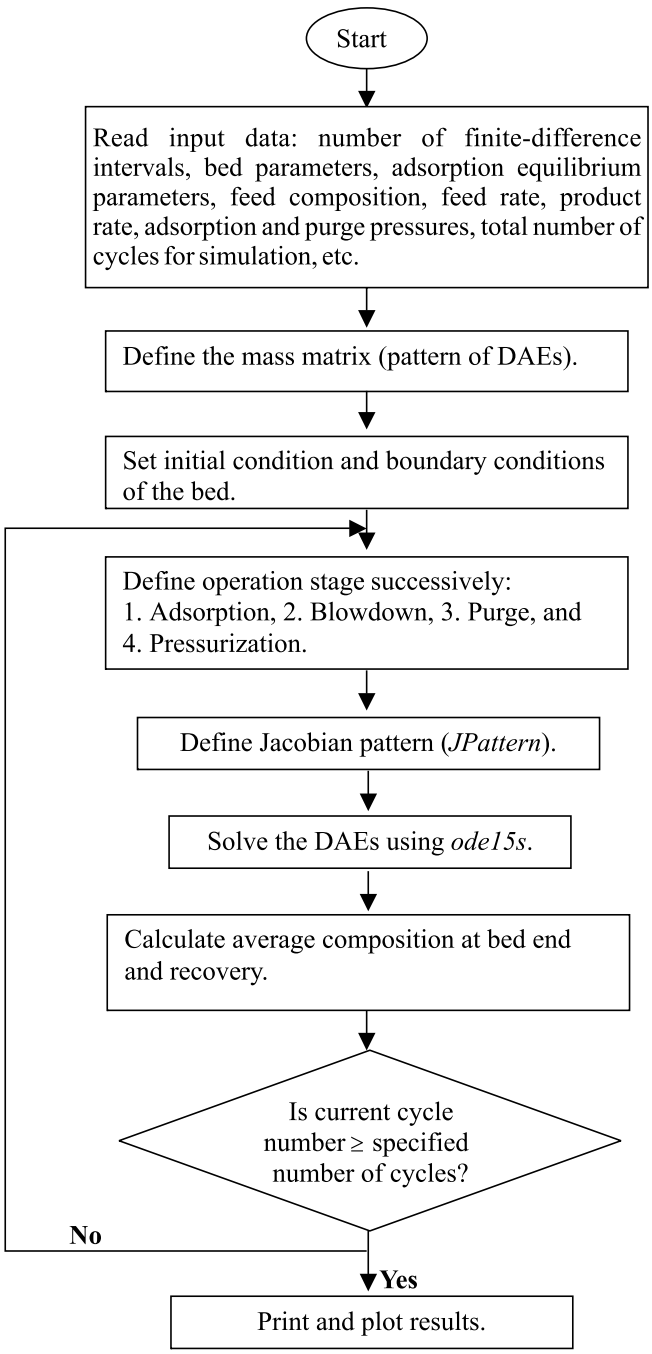

Figure 1. Flow chart of MATLAB® based simulation methodology for PSA

sults match reasonably well with the experimental results reported earlier. In the current study, the parameter sensitivity has been discussed in detail with respect to the experimental data set number 4 of Farooq *et al.*[12]. For this data set, the values of feed flow rate, product flow rate, cycle time, and adsorption pressure are 25 cm^3/s, 1.13 cm^3/s, 250 s, and 1.9 atm, respectively.

Cyclic Steady State Behavior of PSA System

As most of the adsorption processes are unsteady state in nature, PSA also does not achieve its steady state in true sense. However, CSS is an important condition as it determines the system behavior in the long run. At CSS, the conditions in each bed at the start and end of each cycle are identical indicating normal production of O_2 [25]. Instantaneous O_2 mole% at the bed end for a typical data set (data set number 4 of Farooq *et al.*[12]) is shown in Figure 3. It can be seen that in the initial stages, there is variation

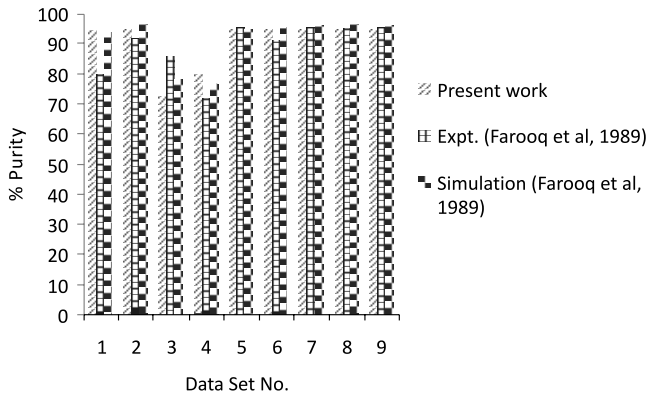

Figure 2a. Percentage purity of O_2 in product

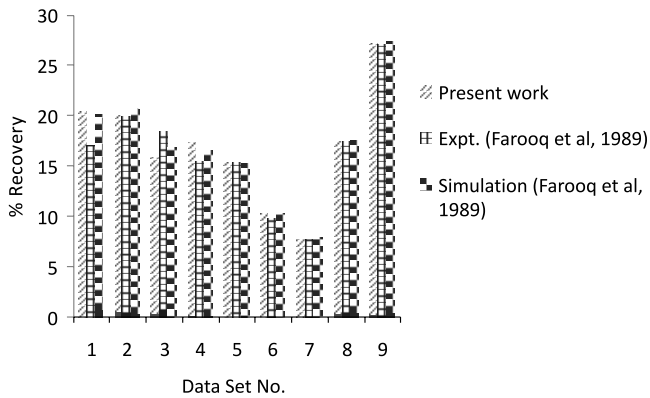

Figure 2b. Percentage recovery of O_2 in product

in the instantaneous O_2 mole% but as the system approaches CSS, the trend of the instantaneous O_2 mole% becomes identical for each cycle.

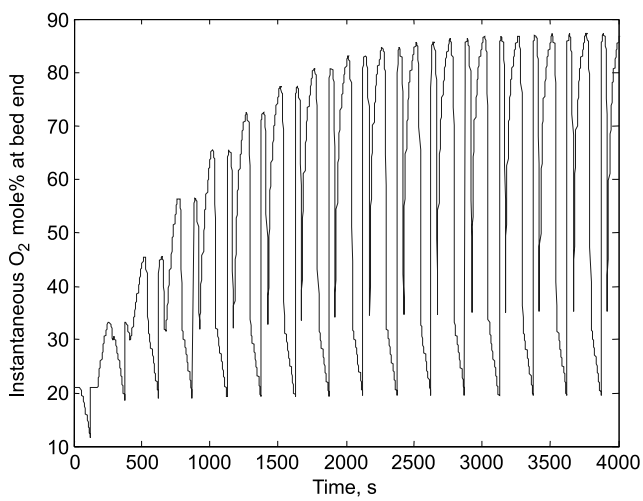

Figure 3. Instantaneous O_2 mole% at the bed end

Figure 4 shows the variation of instantaneous mole% of O_2 during the different steps of a single cycle at CSS. It may be observed that the O_2 mole% increases slightly during the adsorption process, followed by a sharp reduction before the blowdown step. This behavior of reduction in O_2 mole% may be attributed to the saturation of bed after 40 s during the adsorption step. It may be noted that O_2 mole% falls down to 36% in the bed at the end of adsorption step. Further, it decreases almost linearly during blowdown as the change in pressure has been assumed to be linear with time. There is a sharp increase at the beginning of purge step, as the O_2 produced at this stage is of high purity, after which, it decreases slowly with a

sharp reduction just before pressurization. It can be noted that the behavior in the purge step is quite similar to that of adsorption step as the bed is being purged with the same exit composition of the second bed, which is under adsorption stage. It has been reported earlier that all adsorption beds operate under identical conditions with a simple phase difference when the system reaches at CSS[15]. The variation of the composition of the purge fed to the bed over the purge step is precisely the same as the variation of the composition of the product stream from the same bed over the product release step. During pressurization, it increases rapidly in the beginning followed by a plateau phase. The rapid increase in the product purity at the start of pressurization step may be due to the existence of clean bed at the end of purging, resulting in separation of pure O_2 from air. However, the later stage of pressurization indicates that the bed is attaining saturation.

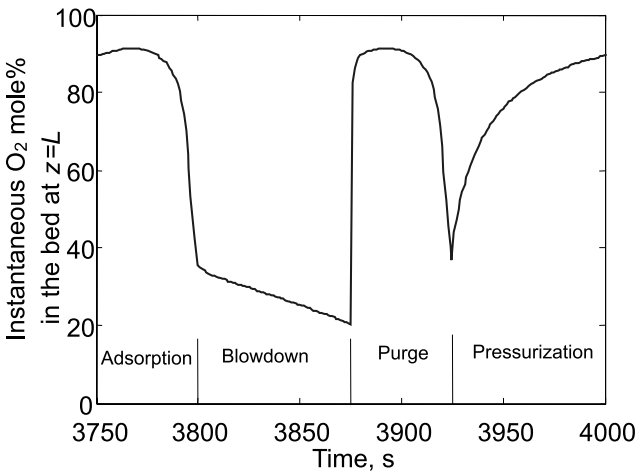

Figure 4. Instantaneous O_2 mole% at bed end during a CSS cycle

Figure 5(a) and (b) show the progress of average product purity and recovery, respectively with respect to cycle number. These two variables were calculated using equations (12) and (13), respectively. It may be observed that the average oxygen purity and recovery become almost constant at 80.4% and 17.3%, respectively after 15 cycles, indicating that the system has achieved CSS. The low average purity of O_2 is due to the rapid fall in O_2 composition after the first 40 s during the adsorption step. It can also be seen that the product purity and recovery plots have the same behavior as the product rate has been kept constant in the current study, and therefore, the recovery is simply proportional to the product purity.

Effect of process parameters

To find the optimum values of the process variables, the effect of these variables on the key parameters of the process need to be studied. Accordingly, adsorption pressure, cycle time, adsorption duration, feed flow rate, and product flow rate have been selected to study the effect on product purity and recovery. The reference process operating conditions were selected corresponding to the data set number 4 of Farooq *et al.*[12]. While studying the effect of various parameters discussed below, only one parameter was changed at a time.

Adsorption pressure

The effect of adsorption pressure on product purity and recovery was investigated to find the optimum pressure as shown in Figures 6(a) and (b), while keeping other parameters constant. As the adsorption pressure increases, the purity and recovery increase because of larger amount of nitrogen adsorbed in the bed. This trend of product purity and recovery is not similar to the previous work by Farooq *et al.*[12] because in the earlier work, the results were obtained for varying feed rate (25 – 50 cm^3/s), whereas in the present study, a constant feed rate of 25.0 cm^3/s was used. A product purity of 95.45% was achieved above an adsorption pressure of 2.5 atm. However, higher pressure will require higher operating cost and there is no significant improvement in O_2 purity above this pressure, therefore, the adsorption pressure may be maintained around this pressure.

Cycle time

While finding the effect of cycle time, the ratio of operation times of all the four steps in a cycle were kept constant, i.e. adsorption, blowdown, purging, and pressurization times were kept in the ratio of 2:3:2:3. Effect of cycle time is shown in Figures 7(a) and (b), from which, it can be observed that once the bed is saturated, i.e. the bed is provided sufficient time for adsorption to

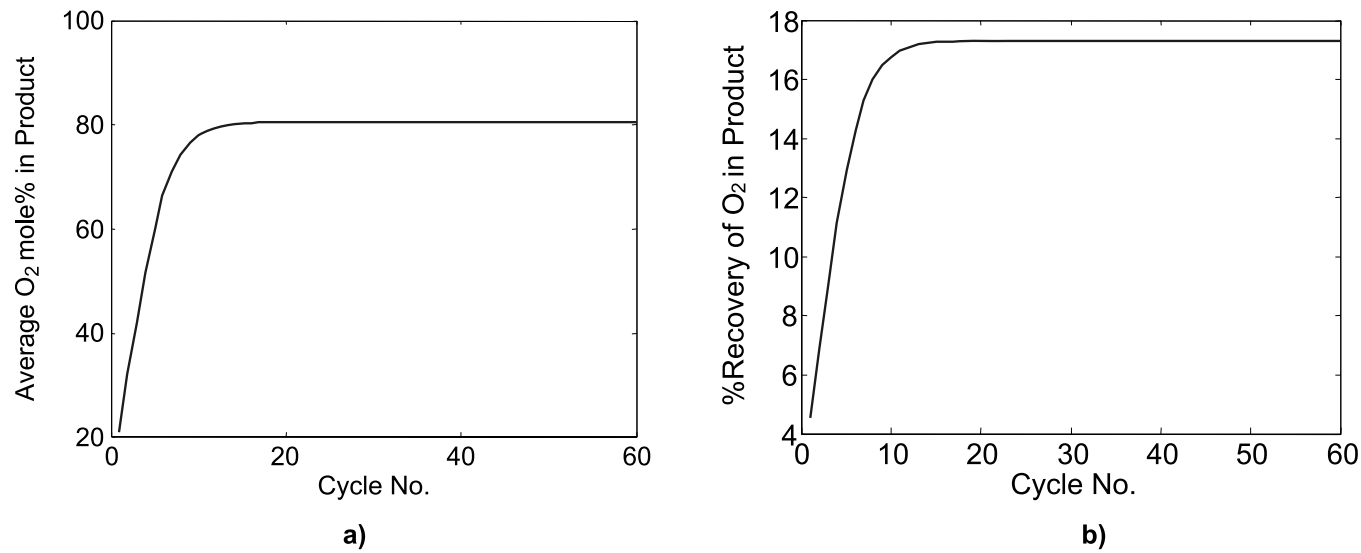

Figure 5. Progress of (a) average product purity and (b) recovery

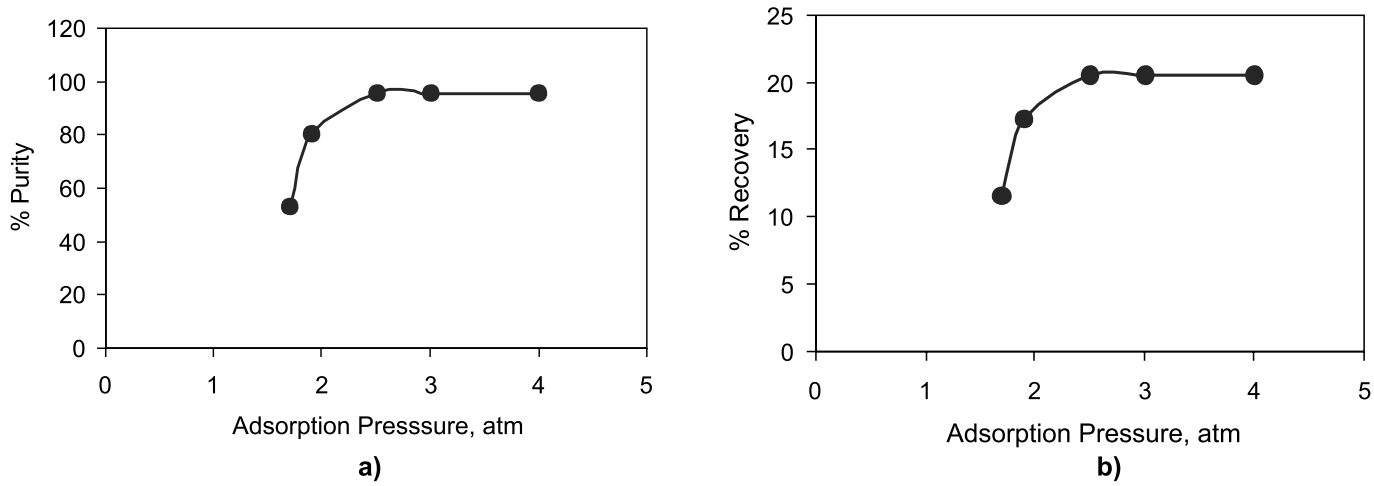

Figure 6. The effect of adsorption pressure on (a) product purity and (b) recovery

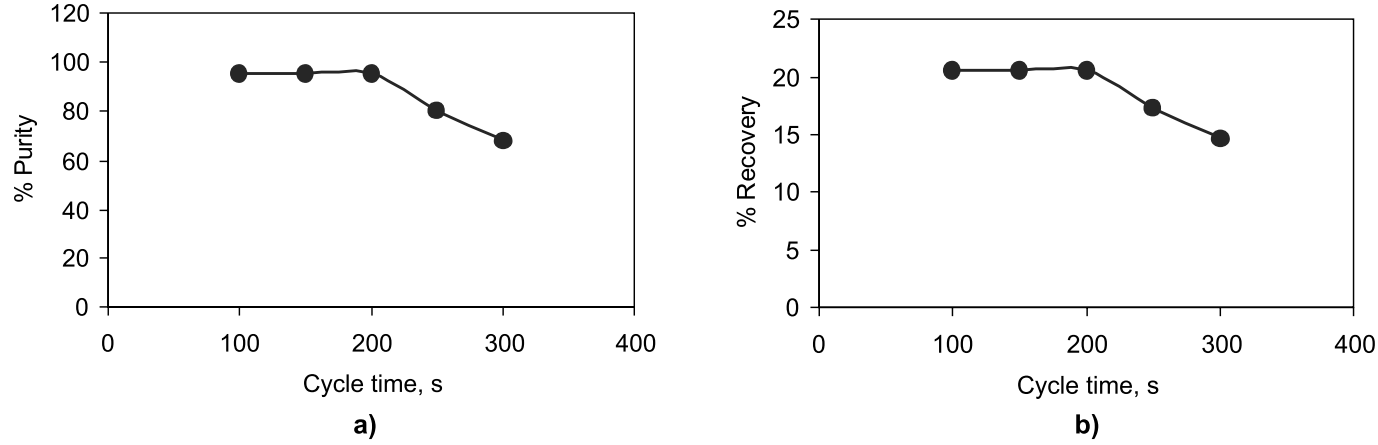

Figure 7. The effect of cycle time on (a) product purity and (b) recovery

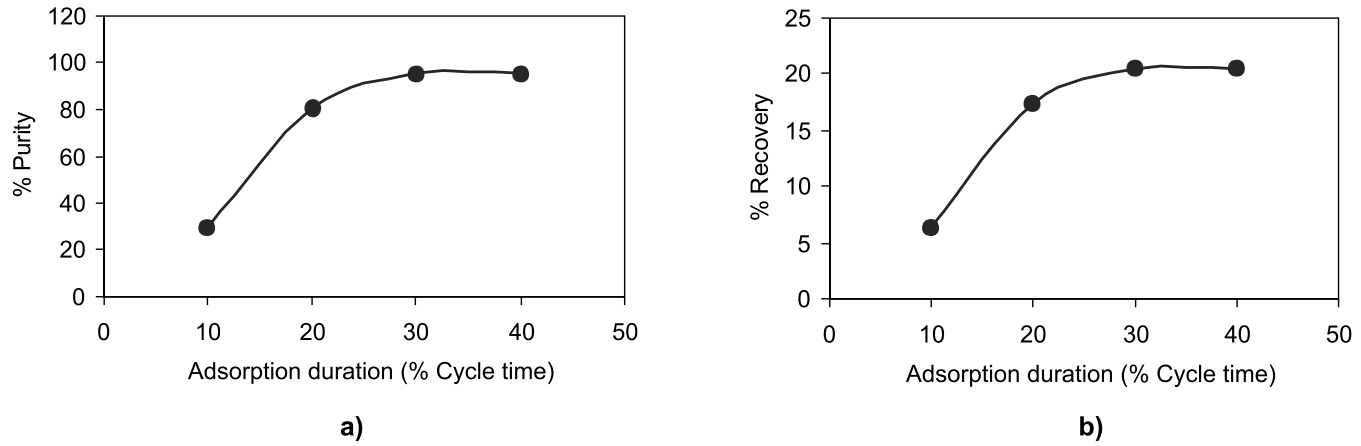

Figure 8. The effect of adsorption duration on (a) product purity and (b) recovery

take place, both product purity and recovery go down. This trend is similar to the results reported earlier[11, 12]. As discussed earlier, the bed gets saturated in 40 s during adsorption; therefore, a cycle time more than 200 s (5 times the adsorption duration) will bring the average purity below maximum achievable. Thus, a cycle time of 200 s or less should yield maximum purity and recovery.

Adsorption duration

While studying the effect of adsorption duration, the total cycle time was assumed to be constant, therefore, all other operation times were also changed. However, the adsorption time and purging time were taken equal; similarly, the purging time and the pressurization time were also taken same. Figures 8(a) and (b) show the effect of adsorption duration on the product purity and recovery, respectively. It can be observed that both purity and recovery increase on increasing the adsorption time and after 30% of total cycle time for adsorption step, both purity and recovery achieve their respective maximum values of 95.45% and 20.55%, respectively. This may be due to the fact that for the increased adsorption time, there is a corresponding increase in purging time and therefore, the bed is in more cleaned condition after purging. The behaviour of Figure 8(a) is in agreement with trend reported earlier[26]. Further, it has been reported that the change in product purity becomes insignificant beyond a certain value of adsorption time.

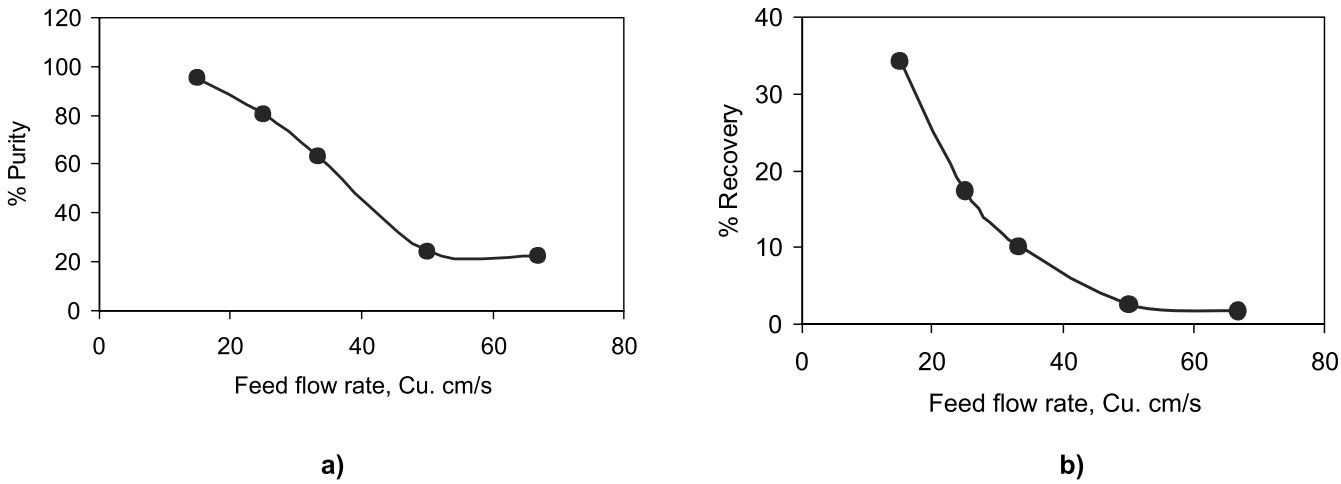

Figure 9. The effect of feed flow rate on (a) product purity and (b) recovery

Feed flow rate

Feed rate directly affects the throughput of the system; however, the actual feed rate should be governed by the desired purity constraint. From Figures 9(a) and (b), it is obvious that increasing the feed rate (or the inlet velocity), reduces the purity and recovery of oxygen in the product as it does not give sufficient residence time for the process to reach its maximum efficiency. As can be seen, the recovery falls rapidly as compared to purity due to both purity decrement and feed flow rate increment, simultaneously.

Product flow rate

Figures 10(a) and (b) show the opposing trends of purity and recovery for the varying product flow rate. On increasing the product flow rate, the purity goes down; however, the recovery follows the reverse trend. This is due to the fact that on increasing the product rate, purging flow rate is reduced thereby reducing the extent of bed regeneration during purging, thus resulting in reduced purity. However, the recovery increases on increasing the product rate, as the total amount of oxygen in the product increases. This trend is not similar to the one reported earlier[12], because in the earlier work, results have been shown only for higher adsorption pressure (4.26 – 4.35 atm), whereas the curves plotted here are at a constant pressure of 1.9 atm only.

The trends of purity and recovery in Figure 6 through Figure 10 show a similar trend to those reported earlier[11, 12]; however, Figure 6(b) shows a different trend as the feed rate was not kept constant in the reported study while studying the effect of adsorption pressure. In Figure 8(b), the trend for the effect of adsorption duration on recovery is also not similar to that reported by Huang *et al.*[17], in which the effect of process parameters has been studied for producing enriched hydrogen from plasma reactor gas by PSA. This is because of the fact that product rate was not kept constant in the abovementioned study; however, in the present study the product rate was kept constant. In most of the cases studied here, recovery is following a similar trend as that of product purity, because for a given product rate and feed rate, the recovery will be proportional to the purity as it is obvious from equation (13). However, it may vary if the product flow rate or feed rate is not kept constant and possibly this may be the reason for a dissimilar trend from earlier studies as mentioned above.

L/D ratio of bed

Length to diameter (L/D) ratio is an important design variable, which affects the flow pattern of the gases, and thereby, the breakthrough curves. While studying the effect of L/D ratio, the bed volume (and therefore the amount of adsorbent) was assumed to be constant. Figures 11(a) and (b) show the effect of L/D ratio on product purity and recovery, respectively. It may be observed that as L/D ratio increases, both product purity and recovery increase monotonically[18] as longer length (and therefore shorter diameter) promotes the plug flow conditions and thereby reduced axial mixing resulting in increased adsorption

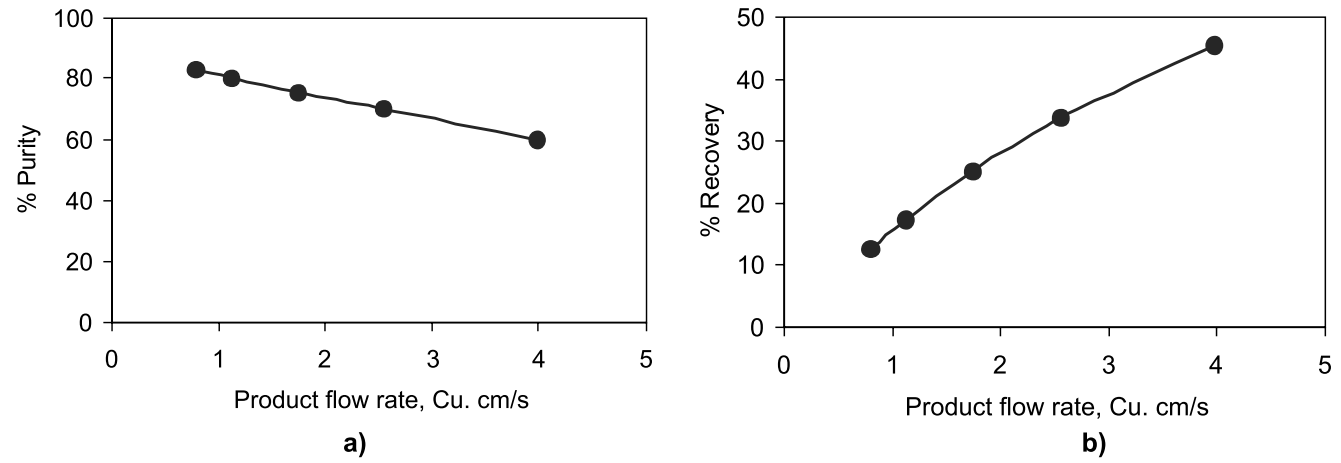

Figure 10. The effect of product flow rate on (a) product purity and (b) recovery

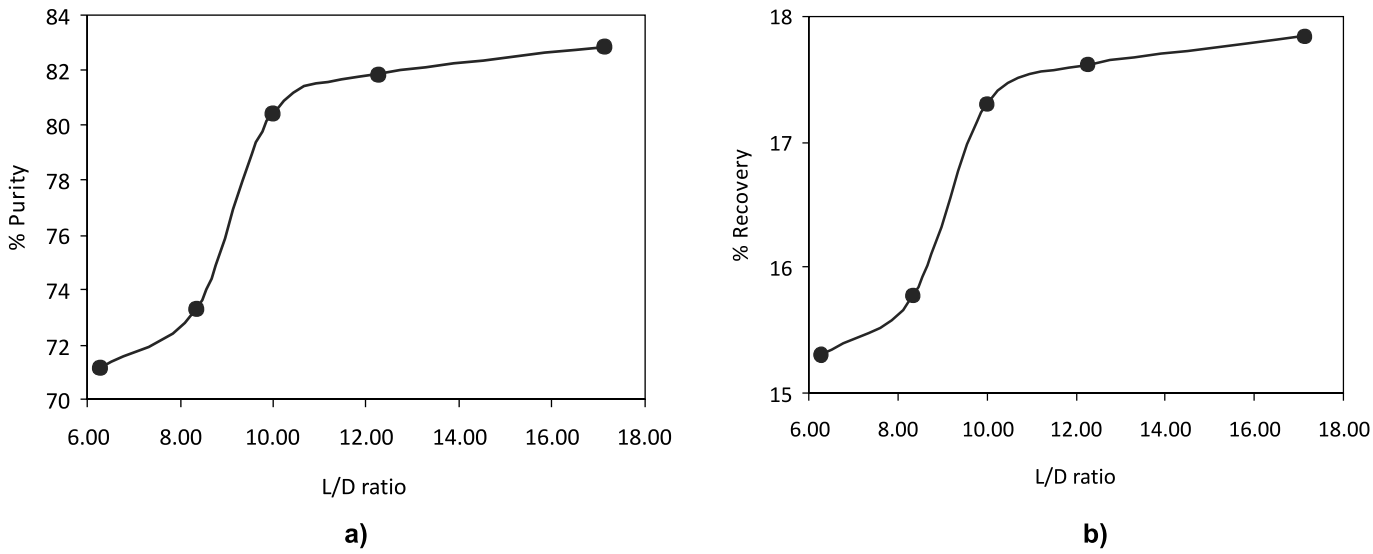

Figure 11. The effect of the L/D ratio on (a) product purity and (b) recovery

during the adsorption step. It may be observed that the value of *L/D* ratio from 8 to 10.5 results in a sharp increase in product purity and recovery values and thereafter, the rate of increase slows down. Beyond an *L/D* ratio of 10.5, there is no significant improvement in purity and recovery of O_2, indicating that an *L/D* ratio of 10.5 is optimum for maximizing the product purity and recovery.

It is important to mention here that increase in *L/D* ratio will also result in increased pressure drop across the bed and at the same time it has its practical limits also due to space limitation. Thus, the increased *L/D* ratio beyond an optimum value will result in both the increased cost of fabrication and the cost of operation. This indicates that PSA operation may be advantageously carried out in a longer tubular unit subject to its operational and economic feasibility. The effect of bed length on product purity was studied earlier[11]; however, the *L/D* ratio presents a more realistic parameter as constant bed volume ensures the same amount of the adsorbent. The effect of the *L/D* ratio on pressure drop across the bed was studied using Blake-Kozeny equation[27] and is shown in Figure 12. The variation of pressure drop was found to be in the range of 0.005 to 0.01 bar for *L/D* ratio of 6 to 17, which is negligible. The pressure drop across PSA bed has also been assumed negligible in earlier studies[28, 29].

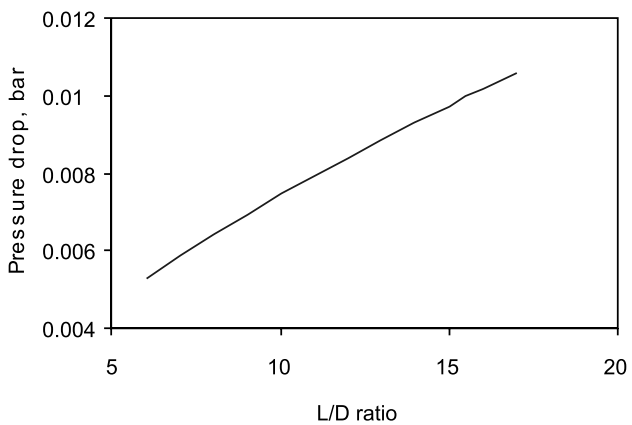

Figure 12. The effect of the L/D ratio on pressure drop

Purge to feed velocity ratio

Purge to feed velocity ratio (*G*) is one of the most important variables in PSA, the increase of which leads to an increase in purity and significant decrease in recovery[18]. The feed throughput can be increased substantially, if a high purge to feed ratio is employed. As per Yang[4], *G* is usually selected in the range of 1.1 to 2. In our study, we have assumed product rate constant, and therefore, the purge velocity was allowed to vary accordingly. This resulted in *G* varying during PSA operation; however, an average value of *G* was calculated to study its effect. It was observed that *G* has significant influence on the number of cycles required to achieve CSS as shown in Figure 13. It can be seen that a value of *G* from 1.5 to 2 requires the minimum number of cycles to achieve CSS (5 to15 cycles, in general).

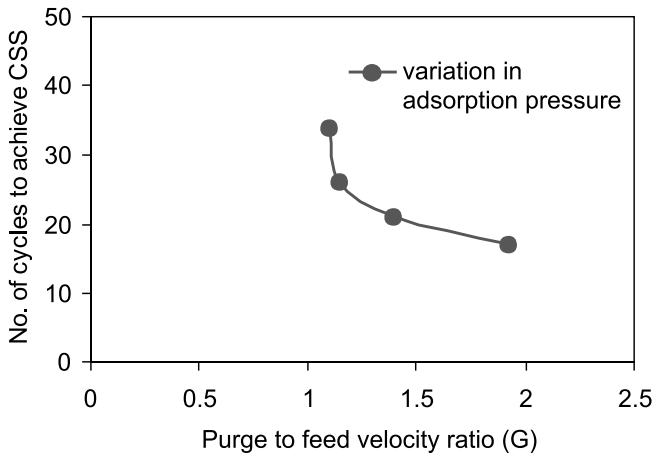

Figure 13. The effect of purge to feed velocity ratio (*G*) on no. of cycles to achieve CSS

Optimal Values of Parameters

As discussed above, the effects of various parameters on the product purity and recovery lead to an optimal set of parameters as shown in Table 2. With these parameters, product purity as high as 95.45% and recovery of 77.27% were achieved as shown in Figure 14(a) and (b), respectively. The design variables are the same as given in Table 1. The system was able to achieve CSS in about 25 cycles only for this case. However, this optimal state has a low feed rate of 15 cm^3/s and thus, the operator needs to maintain a balance between purity, recovery and feed processed. The optimal parameter values should be found on a case to case basis such as market demand, total cost,

etc. It may be noted from Table 2 that the process variables have been optimized to get the maximum purity and recovery both. Further, purging duration was fixed at a constant value of 40% of the total cycle time to achieve a higher purity. At the same time, the product rate of 2.55 cm^3/s and adsorption pressure of 2.5 atm were fixed. The adsorption pressure used was in the range of experimental results of 1.48 to 4.35 atm reported by Farooq *et al.*[12].

In order to see the effect of productivity on power consumption, relationship used by Kearns and Webley[30] was used. The values of the estimated power consumption and productivity for the experimental sets of Farooq *et al.*[12] are given in Table 3. A curve has been plotted between power consumption and productivity shown in Figure 15. It may be observed from Figure 15 that productivity and power consumption are maximum at the same point but minimum power consumption and maximum productivity are at the two extremes. This trend is in agreement with the observations of Kearns and Webley[30]. Moreover, these two do not follow a linear relationship indicating that some other factor is also responsible. Obviously, increase in the adsorption pressure increases both power consumption and productivity.

Table 2. Optimal values of process variables

Process variable	Optimal value
Total cycle time	150 s
Adsorption pressure	2.5 atm
Duration of operation stages	
Adsorption	40% of cycle time
Blowdown	10% of cycle time
Purge	40% of cycle time
Pressurization	10% of cycle time
Feed flow rate	15 cm^3/s
Product flow rate	2.55 cm^3/s

CONCLUSIONS

Numerical simulation for the production of oxygen by separation of air using 5A zeolite has been presented for a two bed PSA process. The simulation is based on a program 'PSASOL' developed in MATLAB®. The transient process of PSA has been described by a set of partial differential equations, which were solved using a finite difference method. The simulation results have been validated with the experimental data reported in literature.

For Skarstrom cycle, simulation results showing the effect of adsorption pressure, cycle time, feed flow rate, product flow rate, and *L/D* ratio on product purity and recovery have been studied. It has been found that a longer tubular unit with an *L/D* ratio of 10.5 is advantageous considering purity and recovery, subject to its operational and economic feasibility. Optimum values of process parameters have been proposed to maximize the product purity and recovery. The pressure drop across the bed was found to be in the range of 0.005 to 0.01 bar for *L/D* ratio of 6 to 17, which is negligible. The variation in the number of cycles to achieve a cyclic steady state (CSS) with different values of purge to feed the velocity ratio (*G*) obtained during simulation runs is also shown for the fixed product rate. Moreover, increase in the adsorption pressure increases both power consumption and productivity.

Table 3. Summary of power consumption and productivity for the simulated experimental data sets

Data Set No.	Feed Rate, mmol/s	Adsorption Pressure, atm	Product Rate, mol/s x10^6	Cycle time, s	Power, kJ/mol of feed air	Productivity, mmol product/kg adsorbent-s
1	1.12	1.48	50.45	100	1.03	0.187
2	1.12	1.66	50.45	150	1.35	0.187
3	1.12	1.73	50.45	200	1.47	0.187
4	1.12	1.9	50.45	250	1.75	0.187
5	1.49	2.33	50.45	200	2.37	0.187
6	2.23	3.41	50.45	200	3.64	0.187
7	2.98	4.3	50.45	160	4.48	0.187
8	2.98	4.35	113.84	160	4.53	0.423
9	2.98	4.26	177.68	160	4.45	0.660

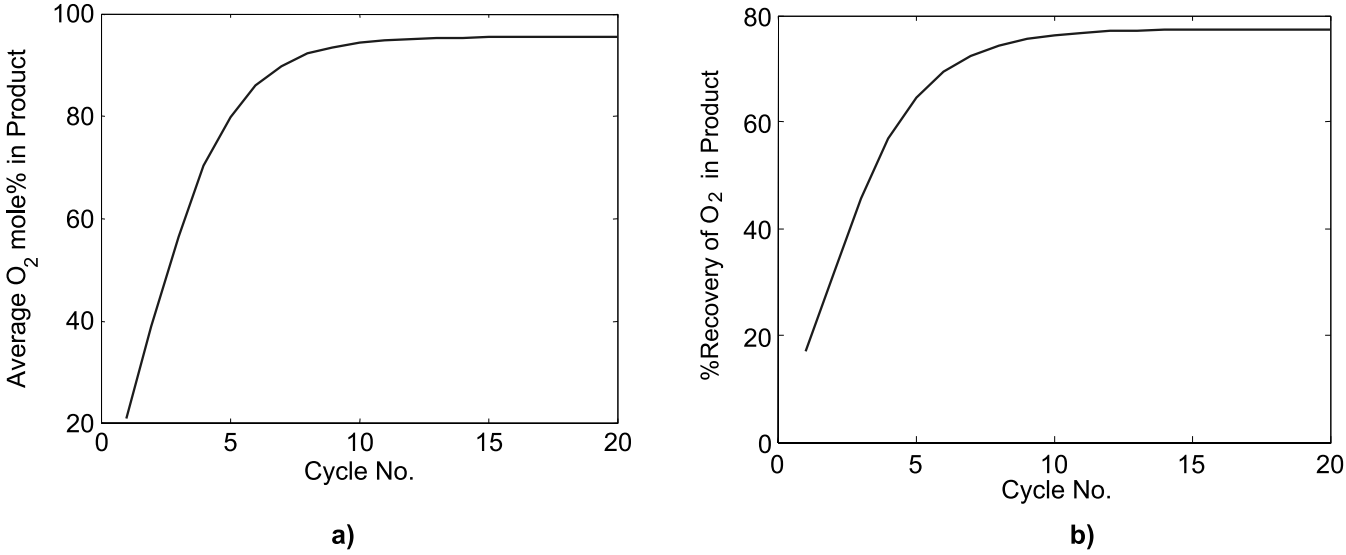

Figure 14. Product purity and recovery of O_2 for the optimal values of parameters

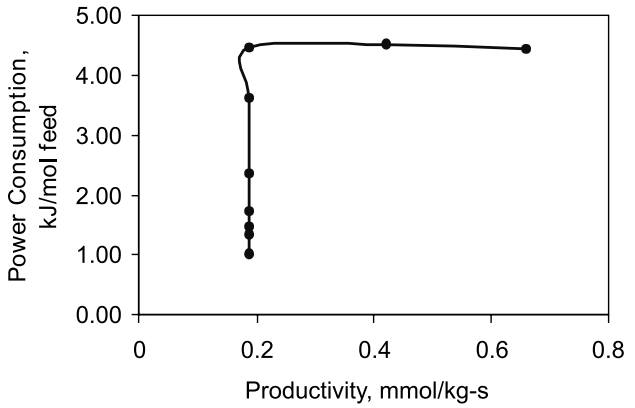

Figure 14. Variation of power consumption with productivity

Based on the simulation results, it can be concluded that for oxygen production from air, operating parameters of the PSA unit with adsorption pressure of 2.5 atm, cycle time of 150 s, feed rate of 15 cm^3/s and product rate of 2.55 cm^3/s yield optimal results. For these optimal conditions, the purity of 95.45% and recovery of 77.3% have been obtained.

Further work can be directed towards optimization of PSA process to minimize the cost, enhance the product purity and/or recovery to find out the optimal values of other design variables, e.g. amount of the adsorbent, pellet size, etc. Such an optimization can also be made to select a suitable adsorbent.

Nomenclature

b_i Langmuir constant for component *i*, m^3/mol
c_i Concentration of component *i* in gas phase, mol/m^3
C Total gas phase concentration, mol/m^3
D_L Axial dispersion coefficient, m^2/s
F_{exit} Molar flow rate of gas at the bed exit, mol/s
F_{feed} Molar flow rate of gas at the bed inlet, mol/s
$F_{product}$ Molar flow rate of product at the bed outlet, mol/s
G Purge to feed velocity ratio
k_i LDF constant for component *i*, s^{-1}
L Bed length, m
$P(P_H,P_L)$ Column pressure (for high pressure step, for low pressure step), N/m^2
q_i Concentration of component i in solid phase, mol/m^3
q_{is} Saturation limit in adsorbed phase for component *i*, mol/m^3
q_i^* Value of q_i in equilibrium with c_i, mol/m^3
t Time, s
t_{ads} Adsorption duration in a cycle, s
v Interstitial velocity in bed, m/s
v_0 Interstitial inlet velocity during pressurization, m/s
v_{OH} Interstitial inlet velocity during high pressure step, m/s
y_{O2} Instantaneous mole fraction of O_2 in gas phase
$y_{O2,\ exit}$ Instantaneous mole fraction of O_2 in gas phase at the bed exit
$y_{O2,\ feed}$ Instantaneous mole fraction of O_2 in gas phase in feed
z Axial distance from column inlet, m

Greek letters

ε Bed voidage

LITERATURE CITED

1. Shuai, X., Cheng, S. & Meisen, A. (1996). Simulation of pressure swing adsorption modules having laminated structure. *Microporous Materials* 5(6), 347 – 355. DOI: 10.1016/0927-6513(95)00070-4.

2. Santos, J. C., Cruz, P., Regala, T., Magalhaes, F. D. & Mendes, A. (2007). High-purity oxygen production by pressure swing adsorption. *Ind. Eng. Chem. Res* 46(2), 591 – 599. DOI: 10.1021/ie060400g.

3. Lee, S. J., Jung, J. H., Moon, J. H., Jee, J. G. & Lee, C. H. (2007). Parametric Study of the Three-Bed Pressure-Vacuum Swing Adsorption Process for High Purity O_2 Generation from Ambient Air. *Industrial and Engineering Chemistry Research* 46(11), 3720 – 3728. DOI: 10.1021/ie061087l.

4. Yang, R. T. (1999). *Gas separation by adsorption processes*. London: Imperial College Press.

5. Jee, J. G., Lee, S. J., Kim, M. B. & Lee, C. H. (2005). Three-bed PVSA process for high-purity O_2 generation from ambient air. AIChE Journal 51(11), 2988-2999. DOI: 10.1002/aic.10548

6. Sircar, S. (2002). Pressure swing adsorption. *Ind. Eng. Chem. Res* 41(6), 1389 – 1392. DOI: 10.1021/ie0109758.

7. Ruthven, D. M. & Farooq, S. (1990). Air separation by pressure swing adsorption. *Gas Separation & Purification* 4, 141 – 148. DOI: 10.1016/0950-4214(90)80016-E.

8. Arvind, R., Farooq, S. & Ruthven, D. M. (2002). Analysis of a piston PSA process for air separation. *Chemical Engineering Science* 57(3), 419 – 433. DOI: 10.1016/S0009-2509(01)00374-8.

9. Jee, J. G., Lee, S. J. & Lee, C. H. (2004). Comparison of the adsorption dynamics of air on zeolite 5A and carbon molecular sieve beds. *Korean Journal of Chemical Engineering* 21(6), 1183 – 1192. DOI: 10.1007/BF02719492.

10. Todd, R. S. & Webley, P. A. (2006). Mass-transfer models for rapid pressure swing adsorption simulation. *AIChE Journal* 52(9), 3126 – 3145. DOI: 10.1002/aic.10948.

11. Ahari, J. S., Pakseresht, S., Mahdyarfar, M., Shokri, S., Zamani, Y., pour, A. N. & Naderi, F. (2006). Predictive Dynamic Model of Air Separation by Pressure Swing Adsorption. *Chemical Engineering & Technology* 29(1), 50 – 58. DOI: 10.1002/ceat.200500226.

12. Farooq, S., Ruthven, D. M. & Boniface, H. A. (1989). Numerical simulation of a pressure swing adsorption oxygen unit. *Chemical Engineering Science* 44(12), 2809 – 2816. DOI: 10.1016/0009-2509(89)85090-0.

13. Hassan, M. M., Ruthven, D. M. & Raghavan, N. S. (1986). Air separation by pressure swing adsorption on a carbon molecular sieve. *Chemical Engineering Science* 41(5), 1333 – 1343. DOI: 10.1016/0009-2509(86)87106-8.

14. Cruz, P., Magalhaes, F. D. & Mendes, A. (2005). On the optimization of cyclic adsorption separation processes. *AIChE Journal* 51(5), 1377 – 1395. DOI: 10.1002/aic.10400.

15. Nilchan, S. & Pantelides, C. C. (1998). On the optimisation of periodic adsorption processes. *Adsorption* 4(2), 113 – 147. DOI: 10.1023/A:1008823102106.

16. Biegler, L. T., Jiang, L. & Fox, V. G. (2005). Recent advances in simulation and optimal design of pressure swing adsorption systems. *Separation & Purification Reviews* 33(1), 1-39. DOI: 10.1081/SPM-120039562.

17. Huang, Q., Malekian, A. & Ei, M. (2008). Optimization of PSA process for producing enriched hydrogen from plasma reactor gas. *Separation and Purification Technology* 62(1), 22 – 31. DOI: 10.1016/j.seppur.2007.12.017.

18. Nikolic, D., Kikkinides, E. S. & Georgiadis, M. C. (2009). Optimization of Multibed Pressure Swing Adsorption Processes. *Ind. Eng. Chem. Res* 48(11), 5388 – 5398. DOI: 10.1021/ie801357a.

19. Shampine, L.F. & Reichelt, M.W. (1997). The MATLAB ODE suite. *SIAM Journal on Scientific Computing*, 18 (1), 1 – 22. DOI: 10.1.1.138.8933.

20. Shampine, L.F., Gladwell, I. & Thompson, S. (2003). *Solving ODEs with MATLAB*, Cambridge University Press, Cambridge, UK.

21. Ruthven, D. M., Farooq, S. & Knaebel, K. S. (1994). *Pressure swing adsorption*. New York, USA: VCH publishers.

22. Tien, C. (1994). *Adsorption calculations and modeling*. Newton, USA: Butterworth-Heinemann.

23. Gomes, V. G. & Yee, K. W. K. (2002). Pressure swing adsorption for carbon dioxide sequestration from exhaust gases. *Separation and purification technology* 28(2), 161 – 171. DOI: 10.1016/S1383-5866(02)00064-3.

24. Agarwal, A., Biegler, L. T. & Zitney, S. E. (2009). Simulation and Optimization of Pressure Swing Adsorption Systems Using Reduced-Order Modeling. *Industrial & Engineering Chemistry Research* 48(5), 2327 – 2343. DOI: 10.1021/ie071416p.

25. Jiang, L., Biegler, L. T. & Fox, V. G. (2005). Design and optimization of pressure swing adsorption systems with parallel implementation. *Computers and Chemical Engineering* 29(2), 393 – 399. DOI: 10.1016/j.compchemeng.2004.08.014.

26. Jain, S., Moharir, A.S., Li, P. & Wozny, G. (2003). Heuristic design of pressure swing adsorption: a preliminary study. *Separation and Purification Technology* 33 (1), 25 – 43. DOI: 10.1016/S1383-5866(02)00208-3.

27. Rota, R. & Wankat, P.C. (1990). Intensification of pressure swing adsorption processes. *AIChE Journal* 36 (9), 1299-1312. DOI: 10.1002/aic.690360903.

28. Takamura, Y., Narita, S., Aoki, J., Hironaka, S. & Uchida, S. (2001). Evaluation of dual-bed pressure swing adsorption for CO_2 recovery from boiler exhaust gas. Separation and purification Technology 24 (3), 519 – 528. DOI: 10.1016/S1383-5866(01)00151-4.

29. Mendes, A.M.M., Costa, C.A.V. & Rodrigues, A.E. (2001). PSA simulation using particle complex models. *Separation and Purification Technology* 24 (1-2), 1 – 11. DOI: 10.1016/S1383-5866(00)00191-X.

30. Kearns, D.T. & Webley, P.A. (2006). Modelling and evaluation of dual reflux pressure swing adsorption cycles: Part II. Productivity and energy consumption. *Chemical Engineering Science* 61 (22), 7234 – 7239. DOI:10.1016/j.ces.2006.07.043.